Russian Journal of Earth Sciences

Distribution of Dissolved Oxygen and Nutrients in Abyssal Waters Flowing into the Brazil Basin, Southwest Atlantic

A. M. Seliverstova[1], O. A. Zuev[*,1], D. I. Frey[1], V. A. Krechik[1], and E. G. Morozov[1]

[1] Shirshov Institute of Oceanology, Russian Academy of Sciences, Moscow, Russia
* **Correspondence to:** Oleg Zuev, qillous@gmail.com

Abstract: The Vema Channel is a deep narrow passage in the South Atlantic and a main path for bottom water which flows northward from the Argentine Basin to the Brazil Basin and after all into the North Atlantic. The thermohaline structure and dynamics in it have been studied for many years. In this study we report our new data on dissolved oxygen and nutrients measurements performed in 2022 at the exit of the Vema Channel. This is the first time that such measurements have been made with high spatial resolution. Data from standard oceanographic sections located near the study area are also analyzed. A significant dependence in the distribution of dissolved oxygen and nutrients on the hydrological structure is shown. Local dissolved oxygen minimum indicates the lower boundary of Circumpolar waters. It was also revealed insignificant temporal variability of nutrients concentration.

Keywords: Vema Channel, abyssal waters, dissolved oxygen, silicate, phosphate, nitrate.

Citation: Seliverstova, A. M., O. A. Zuev, D. I. Frey, V. A. Krechik, and E. G. Morozov (2024), Distribution of Dissolved Oxygen and Nutrients in Abyssal Waters Flowing into the Brazil Basin, Southwest Atlantic, *Russian Journal of Earth Sciences*, 24, ES6004, EDN: GJRPBT, https://doi.org/10.2205/2024es000948

Introduction

Numerous studies have been conducted in the South Atlantic both within the framework of international ocean circulation research programs and in the course of individual researches of different countries. Such interest is explained by the role of the region in the formation and distribution of several water masses that are key for the entire World Ocean [*Holfort and Siedler*, 2001; *Orsi et al.*, 2002]. One of them is Antarctic Bottom Water (AABW, $\theta < 2\,^{\circ}C$ by [*Wüst*, 1936]), which forms in the Weddell Sea and spreads northward in the bottom layer. Through detailed studies, several classifications were proposed dividing AABW into several individual water masses. In our work, we follow the definition [*Reid*, 1989; *Sandoval and Weatherly*, 2001] according to which the AABW consists of Weddell Sea Deep Water (WSDW, $\theta < 0.2\,^{\circ}C$) and Lower Circumpolar Water (LCPW, $\theta < 2\,^{\circ}C$). The characteristic features of WSDW are high density and dissolved oxygen, low temperature and salinity; and characteristic features of LCPW are high values of temperature, silicate, and salinity and low dissolved oxygen relative to the underlying WSDW [*Mantyla and Reid*, 1983].

In its northward flow, the major part of AABW enters the Argentine Basin. The zonally oriented Rio Grande Rise and the Lower Santos Plateau, separating the Argentine and Brazil basins, prevent further free propagation of bottom waters to the north (Figure 1). Water exchange between these basins occurs through the Vema and Hunter channels [*Hogg et al.*, 1999; *Speer and Zenk*, 1993], as well as over the Lower Santos Plateau [*Frey et al.*, 2018]. The densest WSDW passes only through the Vema Channel. Water with $\theta > 0.2\,^{\circ}C$ passes over the Lower Santos Plateau, and water with $\theta > 0.6\,^{\circ}C$ passes through the Hunter Channel [*Sandoval and Weatherly*, 2001]. The Vema Channel is a meridionally located deep-water passage by abyssal currents [*Gamboa et al.*, 1983]. It is more than 700 km long, 15–20 km wide with a depth relative to the terraces forming it of about 500 m, the main sill of the channel is located at 31°12'S, 39°20'W and its depth is 4614 m [*Zenk et al.*, 1993].

Research Article

Received: 10 October 2024
Accepted: 5 November 2024
Published: 30 December 2024

Northward of 29°S the Vema Channel is wider and turns northeastward. For deep narrow passage at about 27°S, 34°W we use the name Vema Extension suggested by [*Zenk and Morozov*, 2007].

Due to its location and structure, the Vema Channel is an excellent object for studying the structure and dynamics of AABW. Different aspects of abyssal circulation, including Ekman layer, Coriolis and bottom friction forces, and potential vorticity conservation were studied in the Vema Channel [*Hogg et al.*, 1982; *Johnson et al.*, 1976; *Reid*, 1989; *Sandoval and Weatherly*, 2001]. During the Deep Basin Experiment, a part of the World Ocean Circulation Experiment [*Hogg et al.*, 1996] and latter studies [*Hogg et al.*, 1999; *McDonagh et al.*, 2002; *Speer and Zenk*, 1993] estimates of velocity and transport of WSDW and LCPW in the Vema Channel were made. The velocity and transport limits are in a wide range, detailed values are given in [*Morozov et al.*, 2021]. Several numerical models were used for calculations of three-dimensional structure of bottom gravity current in the Vema Channel [*Frey et al.*, 2019, 2022; *Wadley and Bigg*, 1996]. Variability of the AABW flow in the channel was studied at different temporal scales [*Campos et al.*, 2021; *Frey et al.*, 2023; *Zenk and Visbeck*, 2013].

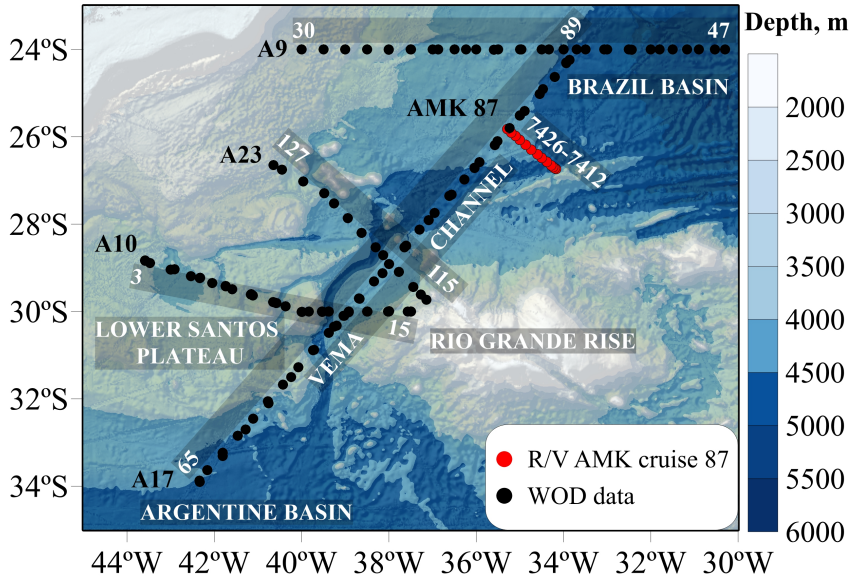

Figure 1. Study area. Red points indicate stations with our measurements in 2022 from 7412 in the southeast to 7426 in the northwest. Black points indicate stations from open databases and sections: A9 (30 and 47 are numbers of the first and last stations in section), A23 (127 and 115), A10 (3 and 15), A17 (65 and 89). The bottom topography is shown according to [*GEBCO Bathymetric Compilation Group 2023*, 2023].

Much less attention has been paid to the study of hydrochemical indicators in the Vema Channel. The values of individual parameters can be found in review papers on the South Atlantic [*Álvarez et al.*, 2014; *Hensen et al.*, 1998; *Holfort and Siedler*, 2001; *Siedler et al.*, 1996; *Vanicek and Siedler*, 2002] or in some oceanographic articles devoted to the hydrology of the Vema Channel [*Hernández-Guerra et al.*, 2019; *McDonagh et al.*, 2002]. However, a detailed description of the hydrochemical structure and its temporal variability in the bottom layer of the channel has not yet been carried out. At the same time, its study and comparison with oceanographic parameters seems interesting both from the point of view of intermediate values between the Argentine and Brazil basins, and for observations of changes in the hydrochemical characteristics in such a complex object as the Vema Channel. Similar studies were carried out in some other deep-water channels, for example, the Vema Fracture Zone [*McCartney et al.*, 1991; *Zuev and Seliverstova*, 2024], the Equatorial Channel [*Andrié et al.*, 2003] and Azores-Gibraltar Fracture Zone [*Krechik et al.*, 2023], which improved the understanding of the temporal and spatial variability of AABW. In this

study we report our new data on dissolved oxygen and nutrients measurements performed in 2022 in the Vema Channel. This is the first time such measurements have been done with high spatial resolution. The goal of the study was to compare the distribution of dissolved oxygen and nutrients with oceanographic parameters of AABW. A comparison of all parameters in the bottom layer on the continental slope and in the deep bed of the Vema Channel was carried out, the presence and position of the oxygen minimum in LCPW were shown, and the spatial and temporal variability of dissolved oxygen and silicate in the channel area was investigated.

Data and Methods

A total of 13 stations were performed within the Vema Channel from 3 to 6 March 2022 in the 87th cruise of the research vessel *Akademik Mstislav Keldysh*. Oceanographic measurements at stations were made with an Idronaut OCEAN SEVEN 320Plus CTD probe (Italy). The lowered probe is equipped with a high-precision temperature-compensated pressure sensor (PA–10X) with an accuracy of 0.01% and a resolution of 0.002% for the entire measurement range (0–100 m), two redundant temperature sensors with a measurement range from −5 to 45 °C, initial accuracy of 0.001 °C, and a resolution of 0.0001 °C. The two redundant conductivity sensors have a measurement range of 0 to 7 S/m, initial accuracy of 0.0001 S/m, and resolution 0.00001 S/m. The currents were measured with a TRDI Workhorse Monitor Lowered Acoustic Doppler Current profiler (LADCP) with a frequency of 300 kHz. The LADCP data were processed using LDEO Software [*Visbeck*, 2002]. Additionally, tidal velocities calculated using the software described in [*Egbert and Erofeeva*, 2002] were taken into account.

Samples for hydrochemical analyzes were taken at the stations with plastic five-liter Niskin bottles of a Carousel Water Sampler system at the depths based on the vertical distribution of potential temperature and salinity. Sampling and determination of hydrochemical parameters were carried out in accordance with accepted methods no later than 6–12 hours after sampling. Dissolved oxygen in seawater was analyzed using the Winkler method modified by Carpenter in 1965 (micromethod) [*Cartenter*, 1965]. Determination of dissolved inorganic silicate was carried out according to the Koroleff method [*Grasshoff et al.*, 2009] with the formation of blue molybdenum complex. When high values of silicate concentration were expected, samples were pre-diluted 1:2 or 1:10 with low-silicate seawater. The sensitivity limit of the element determination was 0.0005 mg/L, the total error of determination was 5.8%. Determination of the concentration of dissolved inorganic phosphate was carried out according to the method of Morphy and Riley [*Grasshoff et al.*, 2009]. The sensitivity limit of the element determination was 0.02 μM/L. Accuracy index (error limits at probability 0.95) 10%. The determination of nitrate was based on the method of reducing them to nitrite with cadmium and measuring calorimetrically [*Grasshoff et al.*, 2009]. The limit of sensitivity of determination of the element was 0.02 μM/L, the total error of determination was 7.4%.

We used additional open data of ship observations from the World Ocean Database, 2018 [*Boyer et al.*, 2018]. The main data are A09, A10, A17 and A23 sections from WOCE and CLIVAR projects. The location of sections is shown in Figure 1.

Results and Discussion

Water structure at the Vema Extension section

Distribution of potential temperature at the Vema Extension section (Figure 2) shows features of AABW before it entered the Brazil Basin. The densest and coldest part of AABW was in the deep bed of the Vema Channel (stations 7413–7415), while the water on the western continental slope was warmer, but still significantly colder than 0.2 °C. The bottom homogeneous layer in the Vema Channel with a thickness of 200–250 m was located from the bottom to depths of about 4450 m, the mean potential temperature was −0.06 °C. At stations 7418 and 7419, the homogeneous bottom layer was absent, the minima bottom potential temperatures were 0.11 °C and 0.05 °C, respectively. On the western continental

slope (stations 7420–7425) the bottom homogeneous layer was about 50 m with a spread of potential temperature values of 0.01–0.05 °C. The dynamic structure was consistent with the distribution of potential temperature. In the deep bed of the Vema Channel there was a flow with velocities higher than 20 cm/s, and on the western continental slope there was a flow with velocities higher than 10 cm/s. At the same time, in the bottom layer at stations 7418–7419 there was a flow with velocities of about 5 cm/s in the opposite direction, which corresponds to the absence of a homogeneous layer and the presence of relatively high potential temperature.

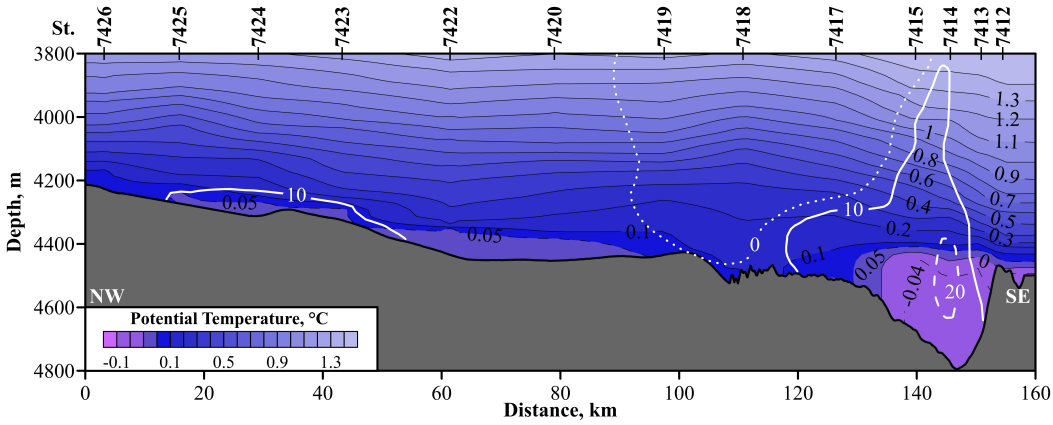

Figure 2. Distribution of potential temperature at the Vema Extension section. The white solid line marks isotach 10 cm/s, the white dashed line marks isotach 20 cm/s, the white dotted line marks isotach 0 cm/s; positive direction is to the northeast, normal to the section. Black lines and numbers at the top axis indicate locations of stations. The bottom topography is shown according to [*GEBCO Bathymetric Compilation Group 2023*, 2023].

The dissolved oxygen concentration was varied from 5.06 to 5.58 mL/L (Figure 3a). The maximum dissolved oxygen concentration was located at 3800 m in the deep bed of the Vema Channel, the minimum was located at 4150 m and 4168 m at stations 7425 and 7424, respectively. The thickness of the local oxygen minimum layer (5.06–5.09 mL/L) was about 50–100 m and this layer was located at depths from 4400 m in the eastern part of the section to 4100 m in the western part. Below this layer, an increase in the dissolved oxygen concentration was observed (on average to 5.09–5.12 mL/L) with a local maximum at the bottom. The silicate concentration was varied from 57.95 µM to 125.17 µM. (Figure 3b). The minimum was located at 3800 m in the deep bed of the Vema Channel, the maximum was at station 7413 from 4400 m to the bottom. At all stations, a uniform increase in the silicate concentration towards the bottom was observed. The distribution of nitrate was similar to the distribution of silicate (Figure 3c). The range of values was varied from 23.75 µM to 32.86 µM; the minimum was at 3800 m at stations 7412–7415, the maximum was in the bottom layer at stations 7413 and 7414. The distribution of phosphate was less uniform (Figure 3d). Absolute values were varied from 1.61 µM to 2.25 µM. Increased phosphate was observed in the bottom layer at stations 7415–7419, as well as at stations 7423–7424.

The main feature of the section is the separation of bottom waters both in the vertical and horizontal directions. Thus, the lower boundary of LCPW is distinguished not only by the conventional isotherm of 0.2 °C, but also by the local oxygen minimum. This minimum is observed at all stations of the section, which indicates the existence of WSDW both in the deep bed of the Vema Channel and on the western continental slope. Also, the oxygen isoline of 5.08 mL/L is correlated with the isolines of 111 µM and 31.5 µM silicate and nitrate, respectively. At the same time, the concentrations of nutrients in the bottom homogeneous layer are varied along the section. As expected, the highest silicate (116–120 µM) and nitrate (32–32.4 µM) are located in the deepest part in the main flow of WSDW (Figure 4). Further, with decreasing depth, the concentration of nitrate is

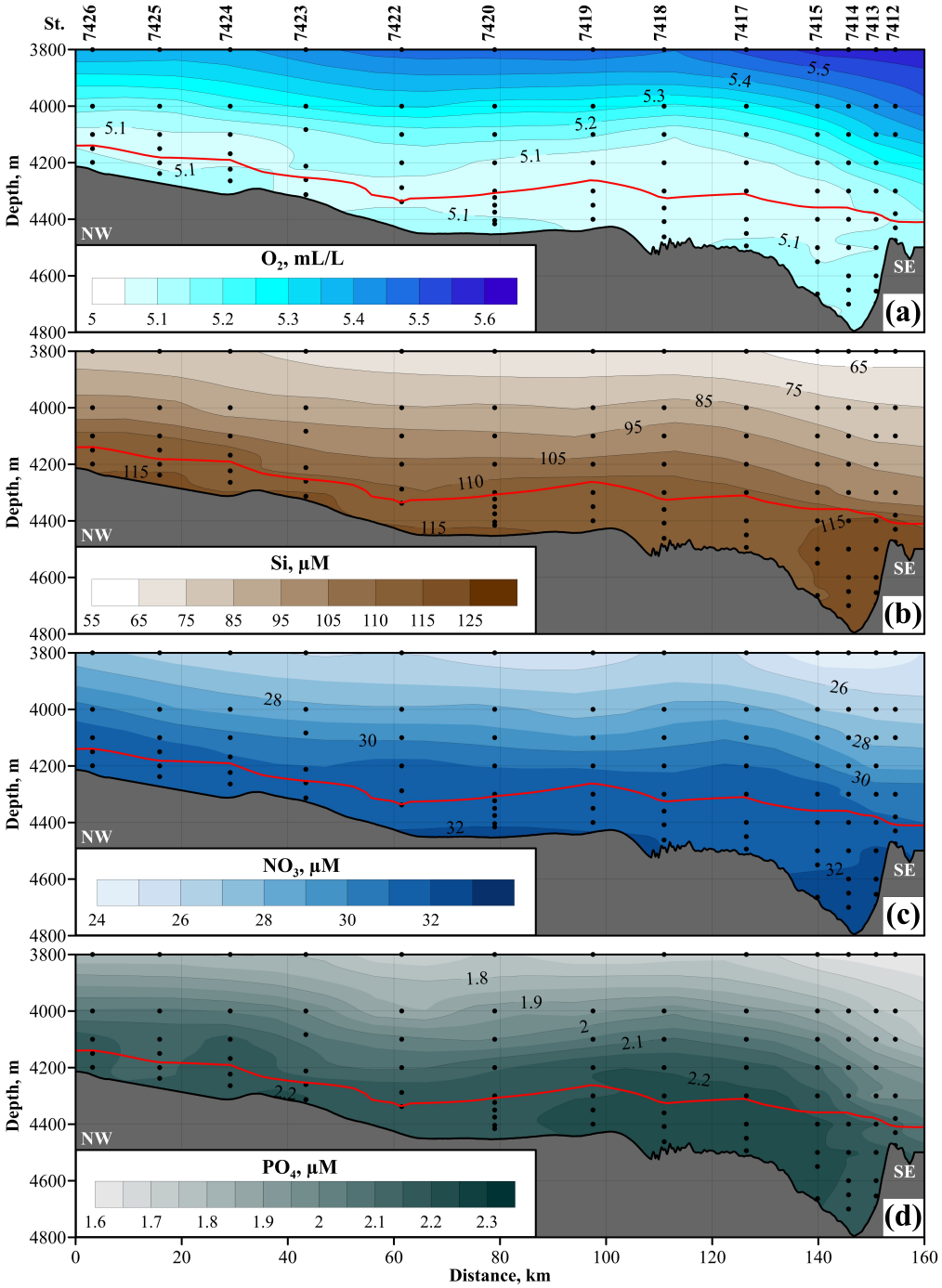

Figure 3. Distributions of (a) dissolved oxygen, (b) silicate, (c) nitrate and (d) phosphate at the Vema Extension section. The red solid line marks isotherm 0.2 °C. Black points and numbers above indicate location of levels and stations. The bottom topography is shown according to [*GEBCO Bathymetric Compilation Group 2023*, 2023].

decreased almost linearly to 31.6 µM, and concentration of silicate is changed in the range of 112–116 µM with the highest value at station 7423. A flow in the northeast direction with velocities exceeding 10 cm/s is also observed here. The distribution of phosphate is noticeably different: the maximum values are at transition stations 7415–7418, the values on the western continental slope and in the deep bed of the Vema Channel are comparable. Probably, this distribution is associated with the reverse flow at the transition stations. Separately, it is necessary to highlight the easternmost station of the section. It is located outside the Vema Channel and the concentrations of all parameters here are

significantly different, which indicates a much smaller volume of WSDW to the east of the Vema Channel.

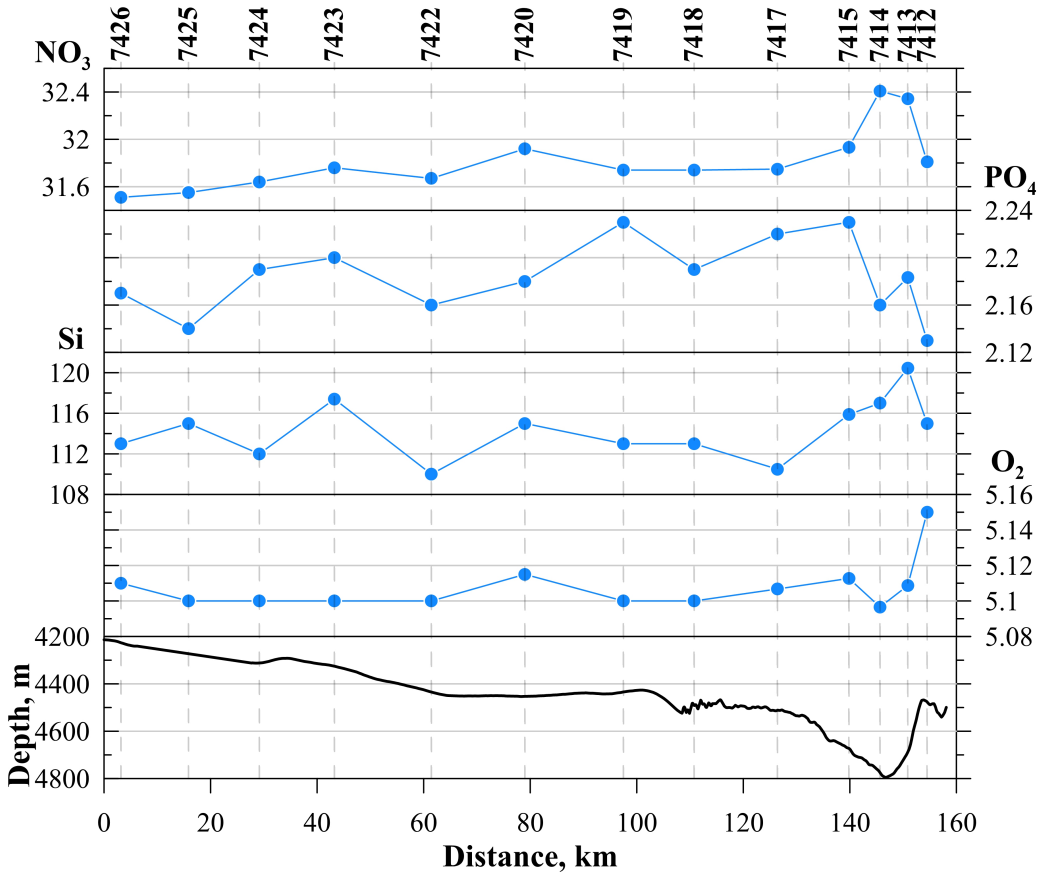

Figure 4. Mean concentrations of dissolved oxygen and nutrients in bottom homogeneous layer. The bottom topography is shown on the lower panel. Data for station 7422 may be incorrect (no measurements at the deepest layer due to technical reasons).

Spatial and temporal variability dissolved oxygen and silicate nearly the Vema Channel

The oxygen minimum in LCPW is observed at other oceanographic sections. Its presence is most clearly expressed in the Argentine Basin: values less than 5 mL/L occupy depths from 3700 m to 4000 m (Figure 5a), respectively, the WSDW thickness here is more than 500 m. A similar pattern is observed in the Vema Channel (station 72). Further, the oxygen minimum disappears, since the stations are located at shallower depths and to the east of the Vema Channel, where WSDW is almost absent. This is clearly seen in sections A10 and A23 (Figure 5b, c): the dissolved oxygen values at the bottom to the east of the Vema Channel are 0.2 mL/L higher than in the western part of the sections. However, even there, an increase in dissolved oxygen toward the bottom is observed only at a few stations, which indicates an insignificant volume of WSDW outside the Vema Channel. On the western continental slope of the Brazil Basin (Figure 5d), separate local oxygen minima are observed, probably related to the division of the bottom water flow into separate jets [*Morozov et al.*, 2022]. The absolute values coincide with the oxygen values over the Lower Santos Plateau, but the layer is much thinner. Further north, the oxygen concentration in the bottom layer is increased, which is consistent with the disappearance of WSDW beyond the Brazil Basin [*Álvarez et al.*, 2014; *Vanicek and Siedler*, 2002]. This configuration is unique, but there are other extremes characterizing LCPW. Just as the LCPW in the Atlantic appears as oxygen minima and silicate maxima because of the contrasting nature of the deep and bottom water there, it appears as a salinity maximum and silicate minimum in the South

Pacific [*Mantyla and Reid*, 1983]. The temporal variability of the oxygen concentration in the bottom layer is extremely weak, local changes can be related to measurement errors or to the intensity of the AABW flow.

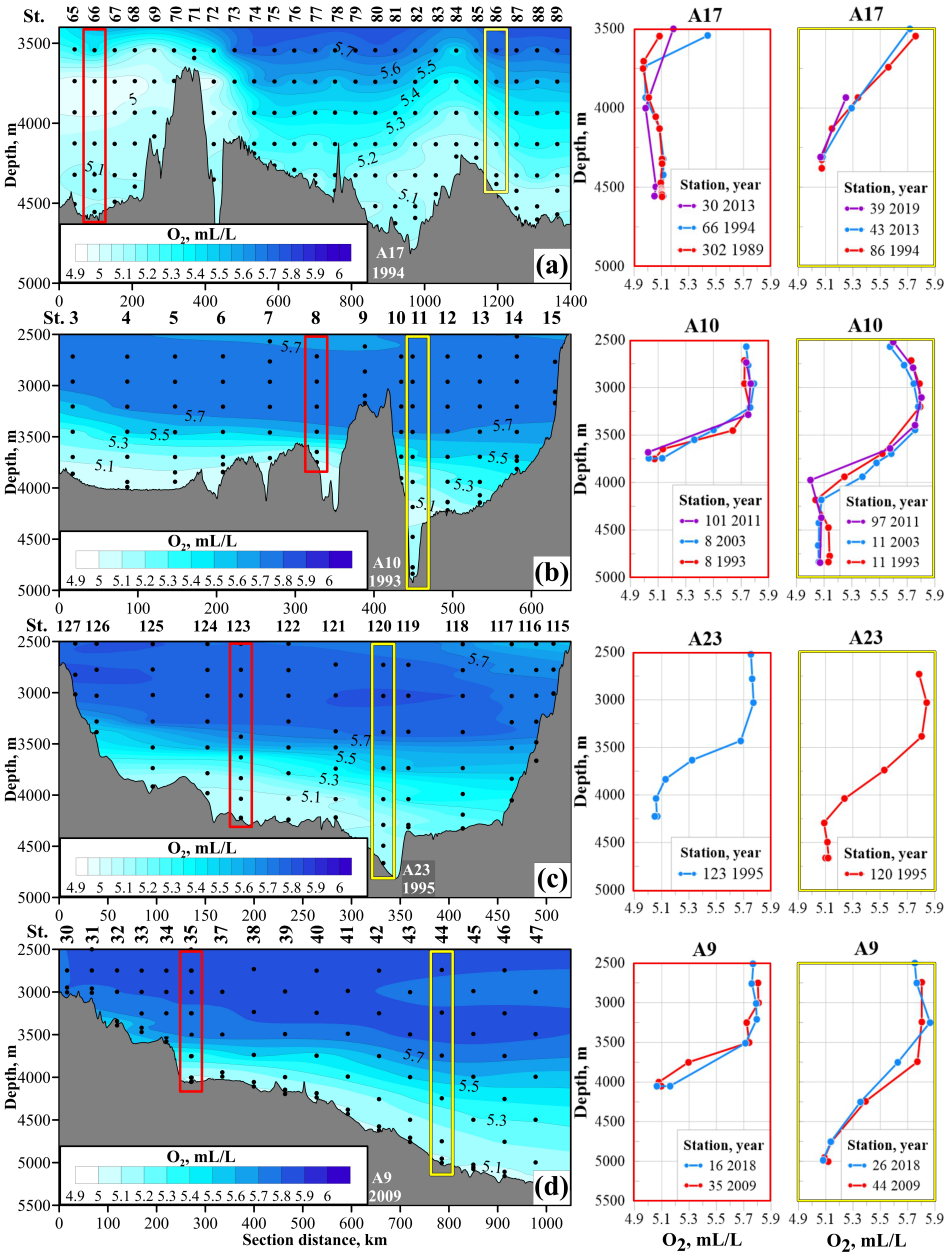

Figure 5. Distribution of dissolved oxygen at (a) A17, (b) A10, (c) A23 and (d) A9 sections. The location of the sections and the first and last station numbers is shown in Fig.1. The bottom topography is shown according to [*GEBCO Bathymetric Compilation Group 2023*, 2023].

The highest silicate concentrations are found near the bottom in the Argentine Basin. Thus, the silicate maximum here is characteristic of WSDW, and not of LCPW as in the Weddell Sea [*Carmack*, 1973; *Mantyla and Reid*, 1983; *Mukhametianov et al.*, 2023]. A significant similarity with the distribution of dissolved oxygen is observed: the presence of its intermediate minimum coincides with the silicate maxima near the bottom, and higher oxygen values correspond to lower silicate concentrations (Figure 6a). The graphs of individual stations for different years show the absence of significant changes of silicate in the bottom layer (Figure 6b, d). The greatest difference is observed in the Argentine Basin, the decrease of silicate was about 8 µM from 1989 to 2013. Such changes may be

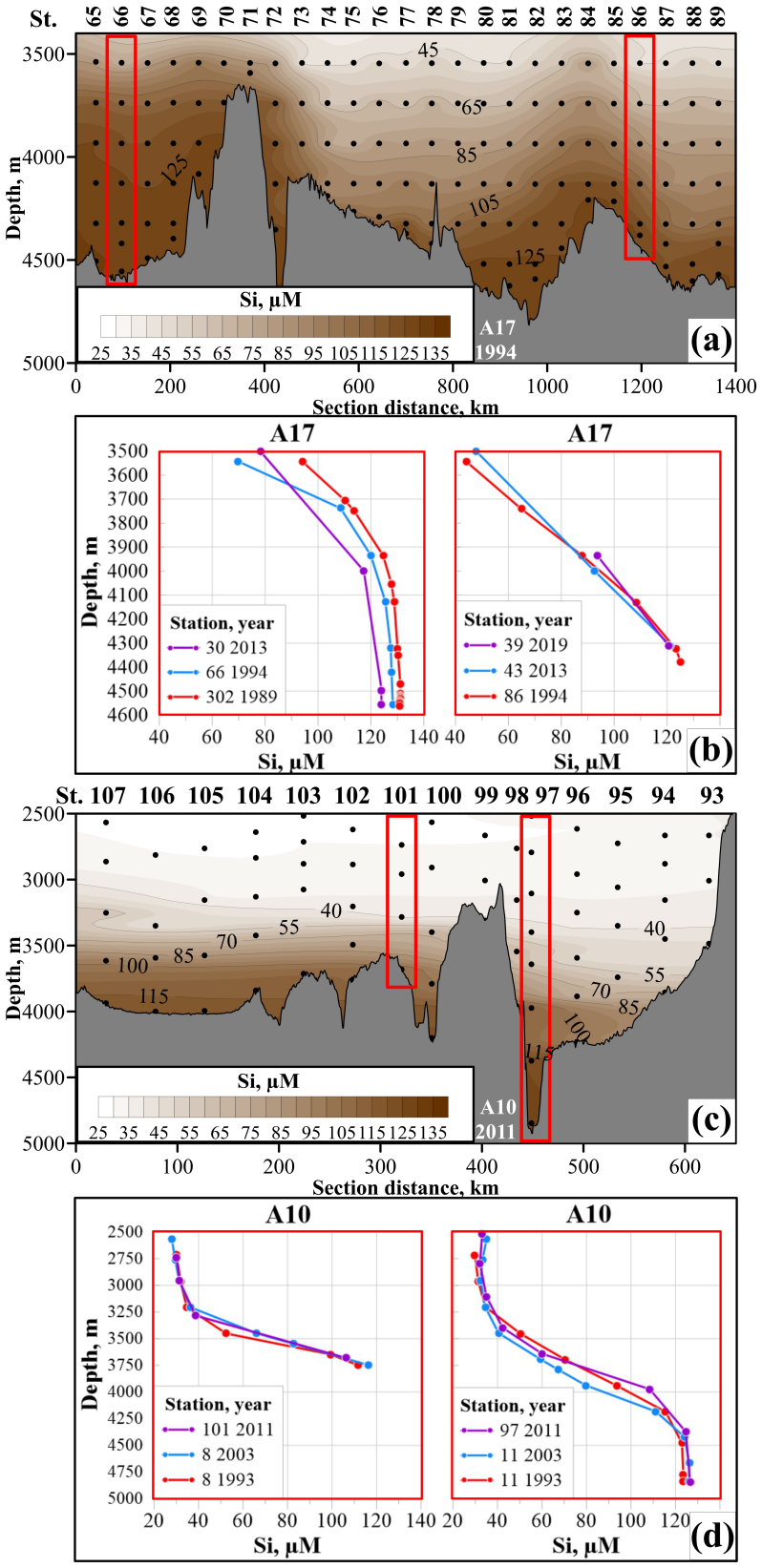

Figure 6. Distribution of silicate at (a) A17 and (c) A10 sections and silicate profiles repeating stations of (b) A17 and (d) A10 sections. The location of the sections and the first and last stations is shown in Fig.1. The bottom topography is shown according to [*GEBCO Bathymetric Compilation Group 2023*, 2023].

caused by different sources of AABW in the Weddell Sea [*Hoppema et al.*, 2015]. At other points, the silicate distribution is almost the same from year to year, so the warming trend of AABW [*Zenk and Morozov*, 2007] is not reflected in the silicate concentration. Station 100 on section A10 (Figure 6c) should be noted separately. It is located in one of the small channels of the Santos Plateau and the silicate concentration here is 124.9 μM, which is only slightly less than at station 97, located in the Vema Channel. The minima of the potential temperature also differ slightly: −0.04 °C against −0.09 °C in the Vema Channel. Thus, it can be assumed that WSDW can flow through individual small channels of the Santos Plateau, but without additional data it is difficult to estimate its volume.

Conclusions

Distribution of dissolved oxygen and nutrients in the abyssal waters near the Vema Channel was analyzed using the in situ data with high spatial resolution. Comparison with potential temperature and current velocities showed significant similarity in distribution even on the horizontal scales of several tens of kilometers. Such water mass tracers as dissolved oxygen and silicate allowed us to identify more accurately the presence and thickness of WSDW over the Vema Extension. Local oxygen minimum on the lower boundary of LCPW was detected in this area. Additional analysis of the open access data showed its strong presence in the Argentine Basin, and poorly noticeable in the Brazil Basin. Silicate concentration complements the pattern of WSDW distribution between the basins. Significant temporal variability in concentrations of dissolved oxygen and nutrients in the bottom layer was not detected. At the same time, significant spatial variability can manifest itself in the presence of high-resolution data, which makes it possible to see additional features of the AABW flow.

Acknowledgments. This work was supported by the Russian Science Foundation grant 24-27-00181.

References

Álvarez, M., S. Brea, H. Mercier, and X. A. Álvarez Salgado (2014), Mineralization of biogenic materials in the water masses of the South Atlantic Ocean. I: Assessment and results of an optimum multiparameter analysis, *Progress in Oceanography*, *123*, 1–23, https://doi.org/10.1016/j.pocean.2013.12.007.

Andrié, C., Y. Gouriou, B. Bourlès, et al. (2003), Variability of AABW properties in the equatorial channel at 35 °W, *Geophysical Research Letters*, *30*(5), https://doi.org/10.1029/2002GL015766.

Boyer, T. P., O. K. Baranova, C. Coleman, et al. (2018), *World Ocean Database 2018*, NOAA Atlas NESDIS 87.

Campos, E. J. D., M. C. van Caspel, W. Zenk, et al. (2021), Warming Trend in Antarctic Bottom Water in the Vema Channel in the South Atlantic, *Geophysical Research Letters*, *48*(19), https://doi.org/10.1029/2021GL094709.

Carmack, E. C. (1973), Silicate and potential temperature in the deep and bottom waters of the western Weddell Sea, *Deep Sea Research and Oceanographic Abstracts*, *20*(10), 927–932, https://doi.org/10.1016/0011-7471(73)90112-5.

Cartenter, J. H. (1965), The Chesapeake Bay Institute technique for the Winkler dissolved oxygen method, *Limnology and Oceanography*, *10*(1), 141–143, https://doi.org/10.4319/lo.1965.10.1.0141.

Egbert, G. D., and S. Y. Erofeeva (2002), Efficient Inverse Modeling of Barotropic Ocean Tides, *Journal of Atmospheric and Oceanic Technology*, *19*(2), 183–204, https://doi.org/10.1175/1520-0426(2002)019<0183:EIMOBO>2.0.CO;2.

Frey, D. I., V. V. Fomin, R. Y. Tarakanov, et al. (2018), Bottom Water Flows in the Vema Channel and over the Santos Plateau Based on the Field and Numerical Experiments, in *The Ocean in Motion*, pp. 475–485, Springer International Publishing, https://doi.org/10.1007/978-3-319-71934-4_29.

Frey, D. I., E. G. Morozov, V. V. Fomin, et al. (2019), Regional Modeling of Antarctic Bottom Water Flows in the Key Passages of the Atlantic, *Journal of Geophysical Research: Oceans*, *124*(11), 8414–8428, https://doi.org/10.1029/2019JC015315.

Frey, D. I., D. Borisov, V. Fomin, et al. (2022), Modeling of bottom currents for estimating their erosional-depositional potential in the Southwest Atlantic, *Journal of Marine Systems*, *230*, 103,736, https://doi.org/10.1016/j.jmarsys.2022.103736.

Frey, D. I., E. G. Morozov, and D. A. Smirnova (2023), Sea level anomalies affect the ocean circulation at abyssal depths, *Scientific Reports*, *13*(1), https://doi.org/10.1038/s41598-023-48074-9.

Gamboa, L. A., R. T. Buffler, and P. F. Barker (1983), Seismic Stratigraphy and Geologic History of the Rio Grande Gap and Southern Brazil Basin, in *Initial Reports of the Deep Sea Drilling Project*, *72*, U.S. Government Printing Office, https://doi.org/10.2973/dsdp.proc.72.119.1983.

GEBCO Bathymetric Compilation Group 2023 (2023), The GEBCO_2023 Grid - a continuous terrain model of the global oceans and land, https://doi.org/10.5285/f98b053b-0cbc-6c23-e053-6c86abc0af7b.

Grasshoff, K., K. Kremling, and M. Ehrhardt (Eds.) (2009), *Methods of Seawater Analysis*, 634 pp., Wiley-VCH, Hoboken.

Hensen, C., H. Landenberger, M. Zabel, and H. D. Schulz (1998), Quantification of diffusive benthic fluxes of nitrate, phosphate, and silicate in the southern Atlantic Ocean, *Global Biogeochemical Cycles*, *12*(1), 193–210, https://doi.org/10.1029/97GB02731.

Hernández-Guerra, A., L. D. Talley, J. L. Pelegrí, et al. (2019), The upper, deep, abyssal and overturning circulation in the Atlantic Ocean at 30 °S in 2003 and 2011, *Progress in Oceanography*, *176*, 102,136, https://doi.org/10.1016/j.pocean.2019.102136.

Hogg, N. G., P. Biscaye, W. Gardener, et al. (1982), On the transport and modification of Antarctic bottom water in the Vema Channel, *Journal of Marine Research*, *40*, 231–263.

Hogg, N. G., W. B. Owens, G. Siedler, and W. Zenk (1996), Circulation in the Deep Brazil Basin, in *The South Atlantic*, pp. 249–260, Springer Berlin Heidelberg, https://doi.org/10.1007/978-3-642-80353-6_13.

Hogg, N. G., G. Siedler, and W. Zenk (1999), Circulation and Variability at the Southern Boundary of the Brazil Basin, *Journal of Physical Oceanography*, *29*(2), 145–157, https://doi.org/10.1175/1520-0485(1999)029<0145:CAVATS>2.0.CO;2.

Holfort, J., and G. Siedler (2001), The Meridional Oceanic Transports of Heat and Nutrients in the South Atlantic, *Journal of Physical Oceanography*, *31*(1), 5–29, https://doi.org/10.1175/1520-0485(2001)031<0005:TMOTOH>2.0.CO;2.

Hoppema, M., K. Bakker, S. M. A. C. van Heuven, et al. (2015), Distributions, trends and inter-annual variability of nutrients along a repeat section through the Weddell Sea (1996-2011), *Marine Chemistry*, *177*, 545–553, https://doi.org/10.1016/j.marchem.2015.08.007.

Johnson, D. A., S. E. McDowell, L. G. Sullivan, and P. E. Biscaye (1976), Abyssal hydrography, nephelometry, currents, and benthic boundary layer structure in the Vema Channel, *Journal of Geophysical Research*, *81*(33), 5771–5786, https://doi.org/10.1029/JC081i033p05771.

Krechik, V. A., M. V. Kapustina, D. I. Frey, et al. (2023), Properties of Antarctic Bottom Water in the Western Gap (Azores-Gibraltar Fracture Zone, Northeast Atlantic) in 2021, *Deep Sea Research Part I: Oceanographic Research Papers*, *202*, 104,191, https://doi.org/10.1016/j.dsr.2023.104191.

Mantyla, A. W., and J. L. Reid (1983), Abyssal characteristics of the World Ocean waters, *Deep Sea Research Part A. Oceanographic Research Papers*, *30*(8), 805–833, https://doi.org/10.1016/0198-0149(83)90002-X.

McCartney, M. S., S. L. Bennett, and M. E. Woodgate-Jones (1991), Eastward Flow through the Mid-Atlantic Ridge at 11 °N and Its Influence on the Abyss of the Eastern Basin, *Journal of Physical Oceanography*, *21*(8), 1089–1121, https://doi.org/10.1175/1520-0485(1991)021<1089:EFTTMA>2.0.CO;2.

McDonagh, E. L., M. Arhan, and K. J. Heywood (2002), On the circulation of bottom water in the region of the Vema Channel, *Deep Sea Research Part I: Oceanographic Research Papers*, *49*(7), 1119–1139, https://doi.org/10.1016/S0967-0637(02)00016-X.

Morozov, E. G., R. Y. Tarakanov, and D. I. Frey (2021), *Bottom Gravity Currents and Overflows in Deep Channels of the Atlantic Ocean: Observations, Analysis, and Modeling*, Springer International Publishing, https://doi.org/10.1007/978-3-030-83074-8.

Morozov, E. G., O. A. Zuev, D. I. Frey, and V. A. Krechik (2022), Antarctic Bottom Water Jets Flowing from the Vema Channel, *Water*, *14*(21), 3438, https://doi.org/10.3390/w14213438.

Mukhametianov, R. Z., A. M. Seliverstova, E. G. Morozov, et al. (2023), Hydrological Structure and Water Dynamics in the Powell Basin in January-February 2022, *Oceanology*, *63*(4), 472–485, https://doi.org/10.1134/S0001437023040136.

Orsi, A. H., W. M. Smethie, and J. L. Bullister (2002), On the total input of Antarctic waters to the deep ocean: A preliminary estimate from chlorofluorocarbon measurements, *Journal of Geophysical Research: Oceans*, *107*(C8), https://doi.org/10.1029/2001JC000976.

Reid, J. L. (1989), On the total geostrophic circulation of the South Atlantic Ocean: Flow patterns, tracers, and transports, *Progress in Oceanography*, *23*(3), 149–244, https://doi.org/10.1016/0079-6611(89)90001-3.

Sandoval, F. J., and G. L. Weatherly (2001), Evolution of the Deep Western Boundary Current of Antarctic Bottom Water in the Brazil Basin, *Journal of Physical Oceanography*, *31*(6), https://doi.org/10.1175/1520-0485(2001)031<1440:EOTDWB>2.0.CO;2.

Siedler, G., T. J. Müller, R. Onken, et al. (1996), The Zonal WOCE Sections in the South Atlantic, in *The South Atlantic*, pp. 83–104, Springer Berlin Heidelberg, https://doi.org/10.1007/978-3-642-80353-6_5.

Speer, K. G., and W. Zenk (1993), The Flow of Antarctic Bottom Water into the Brazil Basin, *Journal of Physical Oceanography*, *23*(12), 2667–2682, https://doi.org/10.1175/1520-0485(1993)023<2667:TFOABW>2.0.CO;2.

Vanicek, M., and G. Siedler (2002), Zonal Fluxes in the Deep Water Layers of the Western South Atlantic Ocean, *Journal of Physical Oceanography*, *32*(8), 2205–2235, https://doi.org/10.1175/1520-0485(2002)032<2205:ZFITDW>2.0.CO;2.

Visbeck, M. (2002), Deep Velocity Profiling Using Lowered Acoustic Doppler Current Profilers: Bottom Track and Inverse Solutions, *Journal of Atmospheric and Oceanic Technology*, *19*(5), 794–807, https://doi.org/10.1175/1520-0426(2002)019<0794:DVPULA>2.0.CO;2.

Wadley, M. R., and G. R. Bigg (1996), Abyssal Channel Flow in Ocean General Circulation Models with Application to the Vema Channel, *Journal of Physical Oceanography*, *26*(1), 38–48, https://doi.org/10.1175/1520-0485(1996)026<0038:ACFIOG>2.0.CO;2.

Wüst, G. (1936), Schichtung und Zirkulation des Atlantischen Ozeans, Das Bodenwasser und die Stratosphäre, in *Wissenschaftliche Ergebnisse, Deutsche Atlantische Expedition auf dem Forschungs - und Vermessungsschiff «Meteor» 1925-1927*, Walter de Gruyter & Co, Berlin (Germany).

Zenk, W., and E. Morozov (2007), Decadal warming of the coldest Antarctic Bottom Water flow through the Vema Channel, *Geophysical Research Letters*, *34*(14), https://doi.org/10.1029/2007GL030340.

Zenk, W., and M. Visbeck (2013), Structure and evolution of the abyssal jet in the Vema Channel of the South Atlantic, *Deep Sea Research Part II: Topical Studies in Oceanography*, *85*, 244–260, https://doi.org/10.1016/j.dsr2.2012.07.033.

Zenk, W., K. G. Speer, and N. G. Hogg (1993), Bathymetry at the Vema Sill, *Deep Sea Research Part I: Oceanographic Research Papers*, *40*(9), 1925–1933, https://doi.org/10.1016/0967-0637(93)90038-5.

Zuev, O., and A. Seliverstova (2024), Spatial Variability of the Hydrochemical Structure in Bottom Gravity Current in the Vema Fracture Zone, *Russian Journal of Earth Sciences*, https://doi.org/10.2205/2024es000945.